Available online at www.sciencedirect.com
SCIENCE DIRECT
Journal of Insect Physiology 52 (2006) 661–668
Journal of Insect Physiology
www.elsevier.com/locate/jinsphys

The cation-chloride cotransporter, masBSC, is widely expressed in *Manduca sexta* tissues

Christopher M. Gillen*, Cheyne R. Blair, Neal R. Heilman, Margaret Somple, Michael Stulberg, Rhadha Thombre, Nicole Watson, Kathy M. Gillen, Haruhiko Itagaki

Department of Biology, Kenyon College, Gambier, OH 43022, USA

Received 10 January 2006; received in revised form 20 February 2006; accepted 21 February 2006

Abstract

Cation-chloride cotransporters, including the Na–K–Cl cotransporter, play an important role in epithelial ion transport in insects. We have determined the tissue distribution of *Manduca sexta* bumetanide sensitive cotransporter (masBSC), a putative Na–K–Cl cotransporter that was originally cloned from *M. sexta* Malpighian tubules. We developed a polyclonal antibody (M6) against a C-terminal fragment of masBSC. masBSC protein was detected by M6 at an apparent molecular mass of ~220 kDa in *M. sexta* foregut, midgut, hindgut, Malpighian tubule, salivary gland, fat body, trachea, and nerve cord. Higher expression was observed in the foregut than in other tissues. M6 stained the apical membrane of midgut epithelial cells in cross-sections of third instar larvae. The transcript of masBSC was detected by RT-PCR in midgut, Malpighian tubule, hindgut, trachea, nerve cord, and fat bodies. Taken together, these findings demonstrate that masBSC is widely expressed in *M. sexta*. While the specific function of masBSC remains unknown, the wide distribution indicates a role of masBSC in a broad range of tissues.

Keywords: *Manduca sexta*; Ion transport; Protein expression; Na–K–Cl cotransporter; Secretion

1. Introduction

Physiological evidence implicates Na–K–Cl cotransport as an important ion transport pathway in several different insect epithelia (Audsley et al., 1993; Ianowski and O'Donnell, 2001; Leyssens et al., 1994; Xu and Marshall, 1999). For example, in Malpighian tubules of larval *Manduca sexta*, fluid secretion is inhibited by the Na–K–Cl cotransporter inhibitor bumetanide and also by the removal of Na, K or Cl from the basolateral side of the tubule (Audsley et al., 1993). Na–K–Cl cotransport is also important in other insect secretory tissues. For instance, Na–K–Cl cotransport is a primary transport pathway across basolateral membranes of cockroach salivary gland cells (Lang and Walz, 2001). Despite the physiological evidence, there remain uncertainties about the precise role of Na–K–Cl cotransport in insect epithelial salt transport. One important objective is to establish the molecular identity of the transport proteins and determine their membrane localization (apical or basolateral) and individual functional properties.

A recent phylogenetic analysis of the *Drosophila* and *Anopheles* genomes revealed several candidate Na–K–Cl cotransporters (Filippov et al., 2003; Pullikuth et al., 2003). Several clusters of insect genes show similarity to the vertebrate Na–K–Cl (NKCC), K–Cl (KCC) and Na–Cl (NCC) cotransporters, with some insect genes clustering more closely with vertebrate KCCs and others more closely with NKCC and NCC. However, the sequence analysis does not reveal whether the latter group of insect genes encodes proteins with NKCC or NCC activities. One group of insect transporters with similarity to vertebrate NKCC and NCC contains two *Anopheles* genes (GenBank accession nos. CG46536 and CG46505), one *Drosophila* gene (GenBank accession no. CG31547), and the focus of this study, the *M. sexta* gene *Manduca sexta* bumetanide sensitive cotransporter (masBSC) (GenBank accession

*Corresponding author. Tel.: +1 740 427 5399; fax: +1 740 427 5741.
E-mail address: gillenc@kenyon.edu (C.M. Gillen).

0022-1910/$ - see front matter © 2006 Elsevier Ltd. All rights reserved.
doi:10.1016/j.jinsphys.2006.02.010

no. U17344 (Reagan, 1995)). Nomenclature of these invertebrate transporters is not settled. Vertebrate cotransporters are named based on ion requirements rather than inhibitor sensitivities, and masBSC is labeled NKClMse in Filippov et al. (2003) and Pullikuth et al. (2003). Given that we currently do not know the ion requirements of masBSC, we have elected to retain for this manuscript the nomenclature of Reagan (1995).

The complete masBSC gene was initially cloned from the Malpighian tubules of the tobacco hornworm, *M. sexta* (Reagan, 1995). Two transcripts of masBSC were identified on Northern blots of *M. sexta* tissues (Reagan, 1995). A 5.3 kb transcript was found in Malpighian tubule, but not in brain or fat bodies. A 6.2 kb transcript was more abundant in brain than in Malpighian tubule, but was not found in fat bodies. The two transcripts could represent separate homologous genes or splice variants of masBSC.

The possibility of multiple isoforms and splice variants of masBSC invites comparison to vertebrate Na–K–Cl and Na-Cl cotransporters. In vertebrates, a K-independent, thiazide-sensitive, Na–Cl cotransporter is highly expressed in kidney tubules (Gamba et al., 1993; Yang et al., 1996). Two Na–K–Cl cotransporter genes (NKCC1 and NKCC2) have been identified in vertebrate tissues (Haas, 1994; Russell, 2000). NKCC1 is widely distributed and localized on the basolateral membranes of secretory epithelia. NKCC2 is localized on the apical membrane of absorptive cells in the kidney. Both NKCC1 and NKCC2 are sensitive to the loop diuretics, including bumetanide and furosemide. Splice variants of both NKCC1 and NKCC2 have been described and found to have differential expression patterns in mammalian tissues (Payne and Forbush III, 1994; Randall et al., 1997; Vibat et al., 2001).

The function of the protein encoded by masBSC and its possible role in epithelial salt transport has not been determined. As a first step towards characterizing masBSC, we have used RT-PCR, Western blotting, and immunohistochemistry to determine the tissue distribution and cellular localization of masBSC in *M. sexta*.

2. Methods

2.1. Antigen and antibody production

We constructed a bacterial expression plasmid containing a C-terminal fragment of *M. sexta* NKCC in frame with the *Schistosoma japonicum* glutathione-S-transferase (GST) gene in the PGEX-2T vector. First, we amplified by PCR a C-terminal fragment of masBSC (563 bp total, from bp 2493 to 3055) using full-length masBSC (GenBank accession no. U17344, kind gift of Reagan, 1995) as template and gene specific primers (msF3: 5′-ATC GGA GTG CAA AGA GAA GGA CAA, msR3: 5′-GTA GCG ACA TGA CCA CGA GAC G). PCR products were subcloned into the TA TOPO vector (Invitrogen, Carlsbad, CA). A restriction fragment created by cuts with XhoI (2581 bp of masBSC sequence) and HindIII (from the TA TOPO linker sequence) was subcloned into the PGEX-2T vector, resulting in the C-terminal region of masBSC, which codes for 159 amino acids (from 861 to 1020), in frame behind the GST protein. The C-terminal region was chosen for several reasons. The selected region is predicted to be cytoplasmic in models of Na–K–Cl cotransporters, and we hoped that the GST fusion would be soluble in weak detergents and therefore amenable to purification. Also, the cytoplasmic C-terminal region of cation-chloride cotransporters is less well conserved than the predicted transmembrane domains, reducing the possibility that the antigen would produce antibodies that cross-react with other cotransporters (Haas and Forbush III, 1998). There is 45–50% amino acid similarity across this region to *Drosophila* (GenBank accession nos. CG31547 and CG4357) and crab (*Callinectes sapidus*, GenBank accession no. AAF05702) sequences that group with vertebrate NKCC and NCC and only 25% similarity to insect sequences (GenBank accession no. CG5594) that group with vertebrate KCC. Finally, effective antibodies against mammalian Na–K–Cl cotransporters have been generated from C-terminal fusion proteins (Lytle et al., 1995).

Escherichia coli (BL21) were transformed with the GST-masBSC plasmid, and fusion protein production was induced with IPTG. A fusion protein with an apparent molecular weight of ~40 kDa was produced. The fusion protein was not soluble in mild detergent (Triton X-100) and thus could not be purified with a glutathione column. Therefore, we gel-purified the intact fusion protein by excising the band from a Coomassie blue-stained gel. Rabbit polyclonal antiserum was produced by a commercial service (Covance, Denver, PA) according to their standard IACUC-approved protocol. The antiserum was purified on a Protein A spin column (Pierce, Rockford, IL).

We characterized the sensitivity and specificity of the M6 antibody. Serum from rabbits collected before injection of the antigen (pre-immune serum) did not show significant reactivity to *M. sexta* tissues (data not shown). As a preliminary test of the specificity of M6, we measured its reactivity to lysates from *E. coli* expressing the C-terminus masBSC/GST fusion protein construct and controls expressing only the GST protein. Western blots with the purified M6 antibody detected a prominent band at approximately 40 kDa (the predicted size of the fusion protein) in cells expressing the masBSC/GST fusion, but showed no reactivity to bands at 40 kDa in lysates from cells not expressing masBSC. This reactivity was to masBSC and not to its GST partner, because M6 did not detect GST in lysates from cells expressing the control GST construct. We optimized primary and secondary antibody concentrations to minimize non-specific background.

2.2. Transient MasBSC expression in SF9 cells

A masBSC expression vector (pIB-masBSC) was created by subcloning the full-length masBSC cDNA (Reagan, 1995) into the pIB/V5-HIS insect expression vector

(Invitrogen). Sf9 cells were grown in TNM-FH complete media at 27 °C. The pIB-masBSC and pIB vector were transfected into exponentially growing Sf9 cells using lipofectin according to the manufacturer's instructions (Invitrogen). Cells were selected for incorporation of the vector by 10 μg/ml blasticidin. After 2 weeks of selection, cells were collected and lysed in 2% SDS for analysis by western blotting.

2.3. Western blotting

M. sexta were obtained from a commercial supplier (Carolina Biological, NC), fed a standard diet (Hornworm diet, Carolina Biological), and grown to early fifth instar. Larvae were anesthetized on ice. Tissues were collected, taking care to fully extract each tissue to minimize bias due to possible regional expression differences. To make membrane preparations, tissues were homogenized vigorously in ice-cold buffer (1 mM EDTA, 250 mM sucrose) with a motor driven Teflon-glass homogenizer. Samples were spun at 3000 g for 5 min to remove debris and then at 47,800 g for 40–60 min to pellet the membrane fraction. Protein concentrations were determined using the bicinchonic acid method (BCA Reagent, Pierce Chemical, Rockford, IL). Samples were resuspended in homogenizing buffer and stored at −80 °C until use. Whole tissue lysates were prepared by adding approximately equal amounts of tissue into 250 μl of 90 °C Tris sample buffer (50 mM Tris, 10% SDS, 10% glycerol, 1% bromophenol blue, 100 mM DTT) and homogenized with a plastic handheld homogenizing tool. Samples were incubated at 90 °C for 10 min, re-homogenized, incubated for another 5 min and then stored at −20 °C.

Proteins were separated on 7.5% Tris–HCl gels and transferred to PVDF membranes. Blots were blocked for 1 h in phosphate buffered saline with 0.1% Tween 20 (PBT) −7.5% milk, and exposed to primary antibody overnight at 4 °C with gentle agitation. Unpurified antiserum was used at dilutions ranging from 1:5000 to 1:20,000. Purified M6 antibody was used at a 1:1000 dilution of a 1 mg/ml stock solution. Blots were washed 3 times for 15 min in PBT −7.5% milk, 3 times for 15 min in PBT, exposed to HRP-conjugated anti-rabbit IgG secondary antibody (Sigma Chemical, 1:5000–1:20,000 dilution) and the washes were repeated. Detection was by chemiluminescence (Super West Dura, Pierce Chemical). Signals were visualized by digital camera (Chemi-imager 4.0, Alpha Innotech, San Leandro, CA) with exposures ranging from 5 to 60 min. Brightness and contrast of images were optimized using Photoshop 6.0 (Adobe Systems, San Jose, CA).

2.4. Immunohistochemistry

Third-instar *Manduca* larvae were anesthetized on ice before being transected and fixed for at least 12 h in 4% paraformaldehyde in PBS at 4 °C. The fixed tissues were rinsed 6 times for 1 h in PBS, placed in 30% sucrose overnight at 4 °C, and then embedded in TBS Tissue Freezing Medium (Triangle Biomedical Science, Durham, NC). 20 μm transverse sections of the entire body were cut at the level of the midgut using a cryostat (Cryocut 1800, Reichert-Jung) at −20 °C and placed onto gelatin-coated slides.

The slides were washed 3 times for 1 h in PBT, then incubated for 4 h in 10% normal goat serum (NGS) in PBT. Purified M6 antibody was diluted 1:100 in 10% NGS in PBT prior to application on the slides overnight at room temperature. The slides were washed 5 times for 1 h in PBT and 1 h in 10% NGS in PBT, and then goat-anti-rabbit (IgG) secondary antibody linked to alkaline phosphatase (Sigma, 1:500 dilution) was applied overnight at room temperature. Slides were then washed 6 times for 1 hr in PBT and color was developed using a standard NBT/BCIP protocol with 175 μg/ml BCIP and 336 μg/ml NBT dissolved in 100 mM Tris buffer (pH 9.5) with 100 mM NaCl, 50 mM $MgCl_2$, and 0.1% Triton X-100. Color was developed for 10–15 min before the reactions were stopped by washing 3 times for 10 min in Tris buffer (pH 7.4) with 10 mM EDTA. The slides were dehydrated in an ethanol series, then coverslipped in Fluormount (Gurr) and photographed with a digital camera (Nikon) mounted on a compound microscope (EX-41, Olympus). Brightness and contrast of the digital images were adjusted in Photoshop (Adobe). These slides were compared to control slides that were treated as above, except that no primary antibody was applied.

2.5. RT-PCR

Tissues were collected from cold-anesthetized *M. sexta*. RNA was produced using the SV total RNA system (Promega, Madison, WI). Between 1 and 5 μg of total RNA was used in first strand cDNA synthesis reactions (Superscript, Gibco, Gaithersburg, MD).

PCR was performed using gene-specific primers and a set of degenerate primers that amplify invertebrate actin (Towle et al., 1997). Gene specific primers were msF3 and R3 (see above) and msF2 (5′-CTC GCG CCC AAC GTG CTG CTC AT) and msR2 (5′-CGT GCC CGA CTC CTG TTT CTT CTG). PCR reactions contained 45 μl PCR Supermix (Gibco, MD; 22 mM Tris–HCl, pH 8.4, 55 mM KCl, 1.65 mM MgCl2, 220 μM nucleotides, and recombinant Taq DNA polymerase), 1 μl of forward and reverse primer (final concentration 0.5 μM), and 2 μl of cDNA. Negative controls without added cDNA were always included. A "Touchdown" PCR protocol was used. The first 10 cycles were 30 s at 94 °C, 30 s at annealing temperature starting at 55 °C and decreasing in 1 °C increments to 46 °C, and 1 min extension at 72 °C. The remaining 30 cycles were 30 s at 94 °C, 30 s at 45 °C, and 1 min at 72 °C. PCR products were separated on 1% agarose gels, stained with ethidium bromide, and visualized using a digital camera (Chemi-imager 4.0, Alpha-Innotech, San Leandro, CA). PCR products were quantified by

spot-densitometry (Alpha-Ease 5.5, Alpha-Innotech, San Leandro, CA); the integrated density value (IDV) for each band was corrected for the background IDV of an immediately adjacent region of the gel.

2.6. Genomic DNA PCR

Genomic DNA was isolated from *M. sexta* midgut using DNAzol reagent (Invitrogen). PCR was performed using PCR Supermix (as above) with the msF3 and msR3 primers. Thirty five cycles were performed as follows: 94 °C for 25 s, 55 °C for 30 s, 72 °C for 50 s, followed by 7 min at 72 °C.

2.7. Sequencing and sequence analysis

PCR products were excised from agarose gels and purified (QIAquick gel extraction, Qiagen). Sequencing was performed by the Neurobiotechnology Center at The Ohio State University. Sequence analysis was performed using the Lasergene version 3 sequence analysis package (DNAstar, Madison, WI).

3. Results

3.1. masBSC protein expression

M6 antiserum recognized a protein at ~220 kDa in Sf9 cells transfected with masBSC (Fig. 1). The antiserum did not react with bands above 100 kDa in cells transfected with vector alone or in non-transfected Sf9 cells. Two lower molecular weight bands were detected in all three cell lines; we interpret these as non-specific binding of M6 to abundant Sf9 cell proteins. The M6 antiserum does not react with proteins above 100 kDa in rabbit kidney membranes (data not shown). There was some reactivity to bands below 100 kDa in rabbit kidney; possibly due to the secondary antibody reacting with rabbit immunoglobins. In membrane preparations, purified M6 antibody detected bands at about 220 kDa in Malpighian tubule and 4th and 5th instar midguts (Fig. 2). We included a gill membrane sample from green crab, *Carcinus maenas,* on this blot to test for cross-species reactivity and detected a band at approximately 220 kDa. We also observed reactivity to bands with lower apparent molecular weight, such as the ~40 kDa band in 5th instar midgut. In several additional Western blots of membranes preparations, we consistently observed reactivity with a band at ~220 kDa, while the reactivity with bands lower than 200 kDa was variable.

Reactivity of M6 to proteins above 200 kDa was observed in all *M. sexta* tissue lysates that were tested, including trachea, salivary gland, Malpighian tubule, nerve cord, midgut, foregut, hindgut, and fat body (Fig. 3). In some tissues, including Malpighian tubule, salivary gland, midgut and foregut, M6 also reacted with proteins at about 90 kDa. Reactivity was greatest in the foregut and lowest in the trachea. Equal loading of protein on this blot was confirmed by Commassie Blue staining. We repeated this experiment with an independent set of tissue preparations, and again observed the highest level of staining in the foregut.

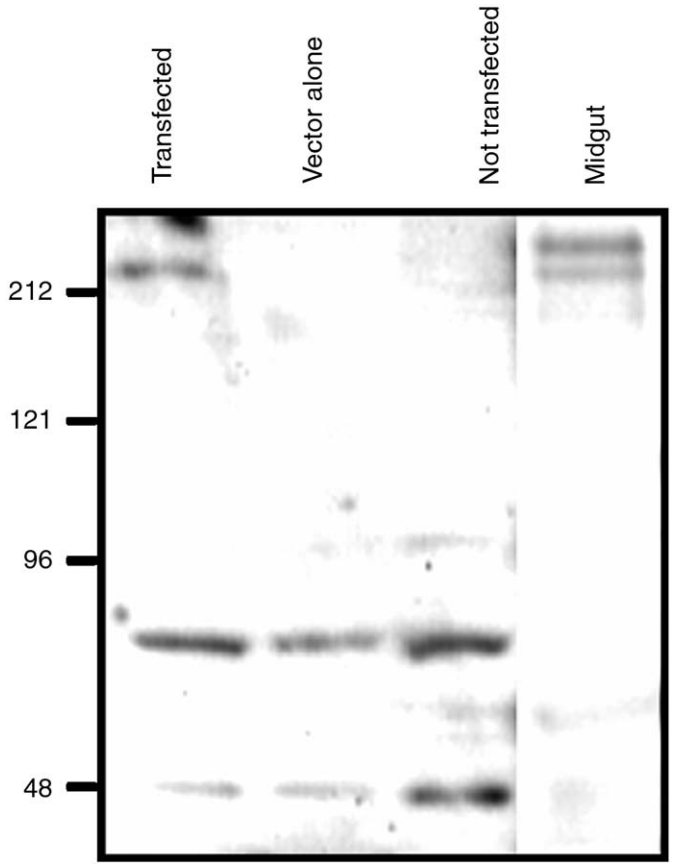

Fig. 1. Western blot of Sf9 cell lysates and *M. sexta* midgut membranes using the M6 antiserum. Numbers on the left indicate migration of molecular mass standards (kDa, Bio-Rad). Detection of chemiluminescence was 60 min for Sf9 lysate lanes and 5 min for midgut membranes run on the same blot.

3.2. masBSC mRNA expression

We used two sets of primers in reverse-transcriptase PCR experiments designed to amplify masBSC mRNA from *M. sexta* tissues. A band of the predicted size (563 bp) was amplified by the msF3/R3 masBSC-specific primers in RT-PCR reactions using RNA isolated from midgut, Malpighian tubule, hindgut, trachea, nerve tissue, and fat bodies ($n = 3$, Fig. 4). This experiment was performed three times with separate sets of tissue. A very faint band was seen in one negative control reaction, but no band was seen in the negative control for the other two trials. Spot densitometry confirmed that bands with intensity greater than the negative control were present for all tissues (Table 1). These data cannot be used to compare expression levels among tissues because the PCR conditions for amplification of both masBSC and actin were not quantitative. PCR products from hindgut, midgut, Malpighian tubule, and

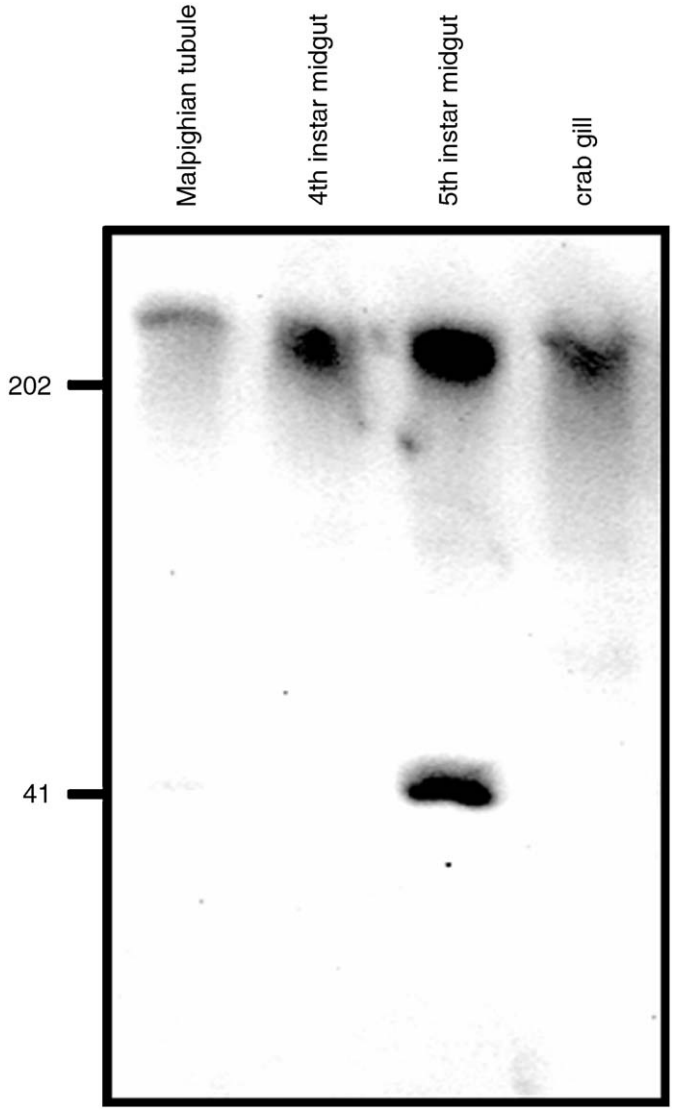

Fig. 2. Western blot of membrane preparations using purified M6 antibody. Numbers on the left indicate migration of molecular mass standards (kDa, Bio-Rad). Equal amounts of *M. sexta* Malpighian tubule, 4th instar midgut and 5th instar midgut were loaded, based on protein concentrations determined by the BCA method. Approximately 5-fold higher amount of *C. maenas* gill membrane was loaded.

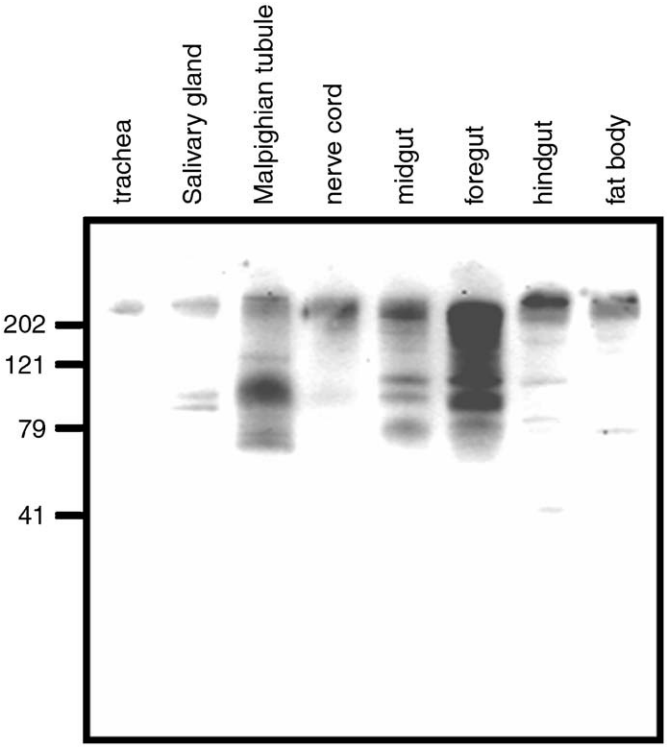

Fig. 3. Western blot of *M. sexta* tissue lysates using purified M6 antibody. Numbers on the left indicate migration of molecular mass standards (kDa, Bio-Rad). Approximately equal amounts of protein were loaded for each tissue, and equal loading was verified by staining of the blot with Coomassie blue (not shown).

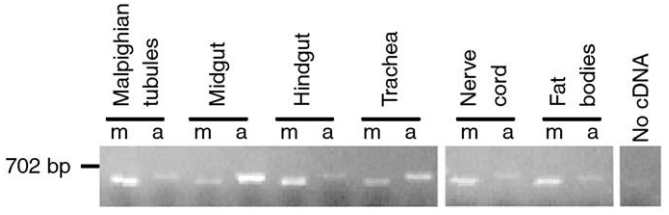

Fig. 4. masBSC and actin RT-PCR products amplified from RNA isolated from *M. sexta* tissues. A DNA size standard is indicated. Lanes represent PCR reactions with cDNAs reverse transcribed from RNA isolated from Malpighian tubules, midgut, hindgut, trachea, ventral nerve cord, and fat bodies using the masBSC-specific primers msF3 and msR3 and degenerate primers against actin (Towle et al., 1997). Products were separated on a 1% agarose gel.

nerve cord were isolated and sequenced. These sequences were more than 99% identical (no more than 2 differences in 353 bp) to each other and were each more than 98% identical (1–5 differences in 353 bp) to the published masBSC sequence (Reagan, 1995). The translated nucleotide sequences matched each other and the translation of the published masBSC sequence exactly over a 129 amino acid peptide. A second set of primers, msF2/R2 did not reliably amplify masBSC from *M. sexta* tissues.

To eliminate the possibility that the 563 bp bands were amplified from contaminant genomic DNA rather than mRNA, we used the msF3 and msR3 primers to amplify *M. sexta* genomic DNA. A PCR product of approximately 1500 bp was detected ($n = 2$) and no band was observed at 563 bp. The genomic PCR product was sequenced and found to match the masBSC sequence but also to contain intron insertions (Fig. 5, GenBank accession no. DQ358048). Thus, the 563 bp bands are not due to amplification of *M. sexta* genomic DNA, but are rather indicative of mRNA expression by each tissue.

3.3. Subcellular localization

No staining was seen in sections incubated with secondary antibody alone (Fig. 6A). In contrast, we observed strong staining on the midgut apical membrane in transverse sections incubated with primary and secondary

Table 1
Spot densitometry of RT-PCR products

Tissue	Integrated density value ($n = 3$)[a]
Malpighian tubule	16859 ± 6284
Midgut	4844 ± 2089
Hindgut	6692 ± 3400
Trachea	2163 ± 1005
Nerve cord	11931 ± 8799
Fat body	18825 ± 5948
Negative control	165 ± 1238

[a]Values are mean ± standard error.

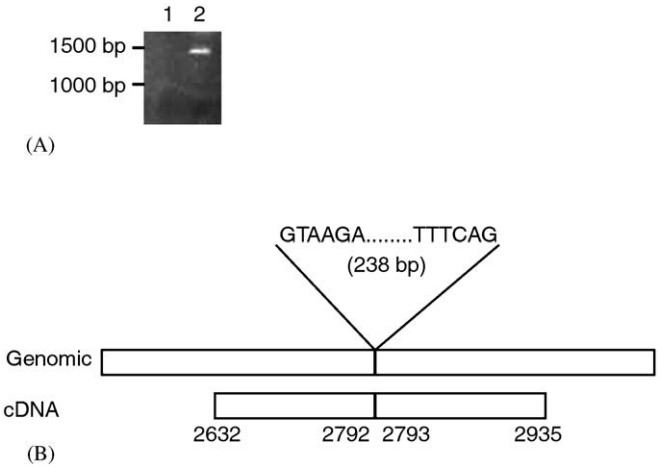

Fig. 5. Alignment of masBSC cDNA and genomic PCR product. Panel A. Fragment of masBSC amplified from genomic DNA using the msF3 and msR3 primers. No product was amplified in control reactions with no DNA added (Lane 1). A ~1500 bp band was amplified in reactions with *M. sexta* genomic DNA (Lane 2). Pabel B. Alignment of masBSC genomic and cDNA sequences. Reliable sequence was obtained for the central region of the genomic PCR product; thus the genomic sequence does not contain matches to the cDNA near the primer binding sites of bp 2493 and 3055 within the open reading frame. The genomic sequence does match the masBSC cDNA sequence (GenBank accession no. U17344) across a 303 bp region except for a 238 intron inserted between bp 2792 and 2793. The genomic sequence does not match the cDNA on each side of the 303 bp region, indicating there are probably additional introns flanking the 303 bp region. The sequence of the genomic PCR product has been submitted to the NCBI database (GenBank accession no. DQ358048).

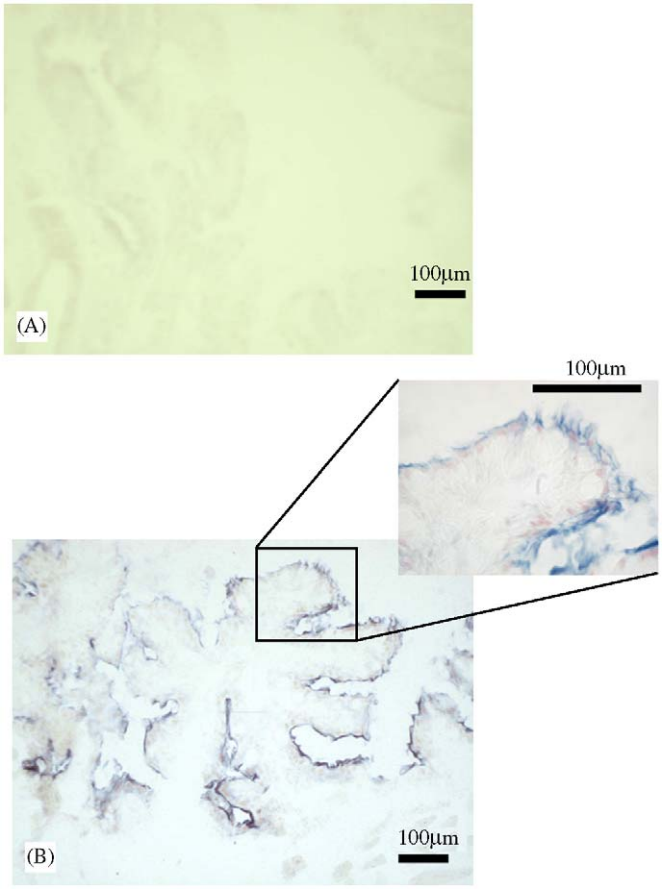

Fig. 6. Staining of *M. sexta* third instar cross-section with purified M6 antibody. No specific staining was seen on negative control sections with no primary antibody applied (Panel A). Immunostaining with purified M6 antibody resulted in robust binding at the apical membrane of midgut epithelial cells (Panel B and inset).

antibody (Fig. 6B). Staining was almost entirely on the cell plasma membrane, with little or no staining in the cytoplasm or intracellular membranes. Staining is primarily on the brush border of columnar cells. In addition to staining on the midgut, some lighter staining was seen on other cell membranes (data not shown).

4. Discussion

We show here that masBSC protein and mRNA are widely distributed throughout *M. sexta* tissues. In midgut cells, we also find masBSC protein expression is isolated to the apical membrane.

The M6 antibody reacts with a band at ~220 kDa in Sf9 cells transfected with masBSC and in *M. sexta* membrane preparations, but does not recognize a band of similar size in mock- or non-transfected Sf9 cells. This result confirms that M6 does detect masBSC and indicates that in transfected cells and in the native tissue, the apparent mass of masBSC is ~220 kDa. In some tissues, we observe reactivity to low molecular weight proteins, but in general this reactivity does not interfere with the ability of M6 to detect proteins at the size expected of a cation-chloride cotransporter.

The observed banding pattern of masBSC on Western blots is consistent with studies that have characterized vertebrate NKCC protein expression. In vertebrate tissues, monoclonal antibodies against NKCC1 detect proteins ranging in apparent mass from 146 to 205 kDa (Lytle et al., 1995). Removal of N-linked oligosaccharides substantially reduces the apparent molecular mass of vertebrate NKCC1. For example, the apparent mass of rabbit parotid gland shifts from ~164 to ~138 kDa after deglycosylation, and 138 kDa is consistent with the molecular mass predicted from the NKCC1 amino acid sequence (Lytle

et al., 1995). The predicted molecular mass of masBSC based on the deduced amino acid sequence is 117 kDa (Reagan, 1995). We find that M6 detects proteins at about 220 kDa in *M. sexta* tissues, suggesting that masBSC, like vertebrate cation-chloride cotransporters, is highly glycosylated. While the size of the protein detected by M6 in *M. sexta* is higher than the apparent mass of NKCC in most mammalian tissues, it is very similar to the apparent mass of NKCC reported in brown trout and salmon (Tipsmark et al., 2002). In some of our Western blots, especially those using crude tissue lysates, the M6 antibody recognized a very broad band or multiple bands rather than a single distinct band. This is a common feature of detection of NKCC proteins on Western blots, and has been observed by other investigators (Lytle et al., 1995; Tipsmark et al., 2002). The presence of multiple bands may result from variable patterns of glycosylation, phosphorylation, or other post-translational modifications. Alternatively, multiple bands might be the result of M6 detecting more than one cation-chloride cotransporter isoform.

M6 detects ~220 kDa proteins from a variety of *M. sexta* tissues, strongly suggesting that masBSC protein is widely distributed in *M. sexta*. A possible explanation of this finding is that masBSC is expressed in the trachea, which are probably present at some level in all of our tissue preparations. However, expression of masBSC in the trachea was much lower than in other tissues. Thus, the observed masBSC expression in midgut, Malpighian tubule and other tissues is probably not due to masBSC expressed on the trachea that penetrate these tissues.

It is possible that the M6 antibody cross-reacts with cation-chloride cotransporters other than masBSC. Theoretically, this is a possibility because it was made against a C-terminal peptide that included regions that are fairly well conserved among Na–K–Cl cotransporters. Also, we find cross-reactivity with ~220 kDa proteins from crab gill, indicating that M6 is not absolutely specific to *M. sexta* masBSC. Indeed, the M6 antibody might be useful for studies of cotransporter proteins in other species. Finally, we sometimes observe multiple bands at ~220 kDa in Western blots, and one explanation for this result is that more than one protein may be detected by the M6 antibody. However, despite the possibility that M6 may recognize other cotransporter isoforms, the RT-PCR results argue that masBSC is indeed widely expressed in *M. sexta*. PCR products amplified using masBSC-specific primers from 4 different tissues were sequenced. All PCR products were essentially identical in nucleotide sequence to masBSC; showing that masBSC is expressed widely in *M. sexta*.

The wide tissue distribution of masBSC detected in this study contrasts somewhat with the findings of others (Filippov et al., 2003; Reagan, 1995). On Northern blots of *M. sexta* tissues, Reagan (1995) found masBSC localized to Malpighian tubule and brain, but not fat bodies. Our findings differ from those of Reagan only in our detection of masBSC in fat bodies, which could be explained by the higher sensitivity of RT-PCR compared to Northern blotting. Filippov et al. (2003) investigated the expression of a *Drosophila* homolog (CG31547) of masBSC by reverse-transcriptase PCR and did not detect the transporter in any larval tissues. This result contrasts with our findings of a broad tissue distribution of masBSC in larval *M. sexta,* and also with the results of Reagan (1995). Although these discrepancies could be due to differences in methodology between studies, it is also possible that there is variation in masBSC expression pattern among insect species. It is intriguing that while cells of Diptera and most other animals have large inward sodium gradients across plasma membranes, cells of Lepidopteran insects have smaller or even reversed sodium gradients (Djamgoz, 1987; Fitzgerald et al., 1996). Therefore, Lepidoptera might have differing needs for a Na-dependent cotransport protein compared to other insects, a possible explanation for species differences in masBSC expression patterns.

The expression pattern of masBSC differs from that of both vertebrate NKCC1 and NKCC2 (reviewed in Russell, 2000). NKCC1 and masBSC both have ubiquitous tissue expression. However, NKCC1 is localized to the basolateral membrane of epithelial cells, while masBSC is on the apical membrane. NKCC2 and masBSC are both expressed on apical membranes of epithelial cells. However, NKCC2 expression is restricted to the kidney while masBSC is expressed widely. This situation is consistent with sequence comparisons of vertebrate and invertebrate cation-chloride cotransporters. The divergence of vertebrate NCC, NKCC1 and NKCC2 apparently occurred within the vertebrate lineage after the separation of vertebrates from the invertebrate line (Pullikuth et al., 2003). Thus, masBSC appears to be equally related to vertebrate NCC, NKCC1, and NKCC2, and it is not surprising that the properties of masBSC do not closely match a particular vertebrate transporter.

We found masBSC protein to be expressed on the apical membrane of midgut epithelia and at high levels in the foregut compared to other tissues. The functional significance of these findings is not known, particularly because there has been no experimental determination of the precise ion requirements of masBSC. One possible role for masBSC would be to participate in Na^+ absorption by moving ions into the cell across the apical membrane. This interpretation is supported by sequence analysis that reveals masBSC is probably a Na^+-dependent cation-chloride cotransporter (Pullikuth et al., 2003), and by measurement of Na^+ absorption across *M. sexta* midgut (Chamberlin, 1990). Functional analysis of masBSC will be required to test the hypothesis that it participates in Na^+ absorption.

Acknowledgments

We thank J. Reagan for the masBSC cDNA. M. Stawiski, S. Mathew, M. Boyce, A. Rowatt, and B. Garratt

contributed to the experimental work described here. Dr. W. Powell and M. Stearns critically read the manuscript. Funding for this work was from the National Science Foundation (IBN-9982375, to C.M.G.) and Kenyon College.

References

Audsley, N., Coast, G.M., Schooley, D.A., 1993. The effects of *Manduca sexta* diuretic hormone on fluid transport by the malpighian tubules and cryptonephric complex of *Manduca sexta*. Journal of Experimental Biology 178, 231–243.

Chamberlin, M.E., 1990. Ion transport across the midgut of the tobacco hornworm (*Manduca sexta*). Journal of Experimental Biology 150, 425–442.

Djamgoz, M.B.A., 1987. Insect muscle: intracellular ion concentrations and mechanisms of resting potential generation. Journal of Insect Physiology 33, 287–314.

Filippov, V., Aimanova, K., Gill, S.S., 2003. Expression of an Aedes aegypti cation-chloride cotransporter and its Drosophila homologues. Insect Molecular Biology 12, 319–331.

Fitzgerald, E., Djamgoz, M., Dunbar, S., 1996. Maintenance of the K+ activity gradient in insect muscle compared in diptera and lepidoptera: contributions of metabolic and exchanger mechanisms. Journal of Experimental Biology 199, 1857–1872.

Gamba, G., Salzberg, S.N., Lambardi, M., Miyanoshita, A., Lytton, J., Hediger, M.A., Brenner, B.M., Hebert, S.C., 1993. Primary structure and functional expression of a cDNA encoding the thiazide-sensitive, electroneutral sodium-chloride cotransporter. Proceedings of the National Academy of Sciences of the United States of America 90, 2749–2753.

Haas, M., 1994. The Na–K–Cl cotransporters. American Journal of Physiology (Cell physiology, 36) 267, C869–C885.

Haas, M., Forbush III, B., 1998. The Na–K–Cl cotransporters. Journal of Bioenergetics and Biomembranes 30, 161–172.

Ianowski, J.P., O'Donnell, M.J., 2001. Transepithelial potential in Malpighian tubules of *Rhodnius prolixus*: Lumen-negative voltages and the triphasic response to serotonin. Journal of Insect Physiology 47, 411–421.

Lang, I., Walz, B., 2001. Dopamine-induced epithelial K+ and Na+ movements in the salivary ducts of *Periplaneta americana*. Journal of Insect Physiology 47, 465–474.

Leyssens, A., Dijkstra, S., Van Kerkhove, E., Steels, P., 1994. Mechanisms of K^+ uptake across the basal membrane of malpighian tubules of *Formica polyctena*: the effect of ions and inhibitors. Journal of Experimental Biology 195, 123–145.

Lytle, C., Xu, J.C., Biemesderfer, D., Forbush III, B., 1995. Distribution and diversity of Na–K–Cl cotransport proteins: a study with monoclonal antibodies. American Journal of Physiology (Cell physiology, 38) 269, C1496–C1505.

Payne, J.A., Forbush III, B., 1994. Alternatively spliced isoforms of the putative renal Na–K–Cl cotransporter are differentially distributed within the rabbit kidney. Proceedings of the National Academy of Sciences of the United States of America 91, 4544–4548.

Pullikuth, A.K., Filippov, V., Gill, S.S., 2003. Phylogeny and cloning of ion transporters in mosquitoes. Journal of Experimental Biology 206, 3857–3868.

Randall, J., Thorne, T., Delpire, E., 1997. Partial cloning and characterization of Slc12a2: the gene encoding the secretory Na+–K+–2C1-cotransporter. American Journal of Physiology 273, C1267–C1277.

Reagan, J.D., 1995. Molecular cloning of a putative Na(+)–K(+)–2Cl-cotransporter from the Malpighian tubules of the tobacco hornworm, *Manduca sexta*. Insect Biochemistry and Molecular Biology 25, 875–880.

Russell, J.M., 2000. Sodium–potassium–chloride cotransport. Physiological Reviews 80, 211–276.

Tipsmark, C.K., Madsen, S.S., Seidelin, M., Christensen, A.S., Cutler, C.P., Cramb, G., 2002. Dynamics of Na(+),K(+),2Cl(−) cotransporter and Na(+),K(+)-ATPase expression in the branchial epithelium of brown trout (*Salmo trutta*) and Atlantic salmon (*Salmo salar*). The Journal of Experimental Zoology 293, 106–118.

Towle, D.W., Rushton, M.E., Heidysch, D., Magnani, J.J., Rose, M.J., Amstutz, A., Jordan, M.K., Shearer, D.W., Wu, W.S., 1997. Sodium/proton antiporter in the euryhaline crab *Carcinus maenas*: molecular cloning, expression and tissue distribution. Journal of Experimental Biology 200, 1003–1014.

Vibat, C.R.T., Holland, M.J., Kang, J.J., Putney, L.K., O'Donnell, M.E., 2001. Quantitation of Na+–K+–2Cl-cotransport splice variants in human tissues using kinetic polymerase chain reaction. Analytical Biochemistry 298, 218–230.

Xu, W., Marshall, A.T., 1999. X-ray microanalysis of the Malpighian tubules of the black field cricket *Teleogryllus oceanicus*: The roles of Na K ATPase and the Na K 2Cl cotransporter. Journal of Insect Physiology 45, 885–893.

Yang, T., Huang, Y.G., Singh, I., Schnermann, J., Briggs, J.P., 1996. Localization of bumetanide- and thiazide-sensitive Na–K–Cl cotransporters along the rat nephron. The American Journal of Physiology 271, F931–F939.